



Modeling of the Coral Microbiome: the Influence of Temperature and Microbial Network

Laís F. O. Lima,^{a,b} Maya Weissman,^{c,*} Micheal Reed,^a Bhavya Papudeshi,^d Amanda T. Alker,^a Megan M. Morris,^{a,*} Robert A. Edwards,^{a,e} Samantha J. de Putron,^f Naveen K. Vaidya,^{c,e} Elizabeth A. Dinsdale^{a,e}

^aDepartment of Biology, San Diego State University, San Diego, California, USA

^bCollege of Biological Sciences, University of California Davis, Davis, California, USA

^cDepartment of Mathematics and Statistics, San Diego State University, San Diego, California, USA

^dNational Center for Genome Analysis Support, Pervasive Institute of Technology, Indiana University, Bloomington, Indiana, USA

^eViral Information Institute, San Diego State University, San Diego, California, USA

^fBermuda Institute of Ocean Sciences, St. George's, Bermuda

ABSTRACT Host-associated microbial communities are shaped by extrinsic and intrinsic factors to the holobiont organism. Environmental factors and microbe-microbe interactions act simultaneously on the microbial community structure, making the microbiome dynamics challenging to predict. The coral microbiome is essential to the health of coral reefs and sensitive to environmental changes. Here, we develop a dynamic model to determine the microbial community structure associated with the surface mucus layer (SML) of corals using temperature as an extrinsic factor and microbial network as an intrinsic factor. The model was validated by comparing the predicted relative abundances of microbial taxa to the relative abundances of microbial taxa from the sample data. The SML microbiome from *Pseudodiploria strigosa* was collected across reef zones in Bermuda, where inner and outer reefs are exposed to distinct thermal profiles. A shotgun metagenomics approach was used to describe the taxonomic composition and the microbial network of the coral SML microbiome. By simulating the annual temperature fluctuations at each reef zone, the model output is statistically identical to the observed data. The model was further applied to six scenarios that combined different profiles of temperature and microbial network to investigate the influence of each of these two factors on the model accuracy. The SML microbiome was best predicted by model scenarios with the temperature profile that was closest to the local thermal environment, regardless of the microbial network profile. Our model shows that the SML microbiome of *P. strigosa* in Bermuda is primarily structured by seasonal fluctuations in temperature at a reef scale, while the microbial network is a secondary driver.

IMPORTANCE Coral microbiome dysbiosis (i.e., shifts in the microbial community structure or complete loss of microbial symbionts) caused by environmental changes is a key player in the decline of coral health worldwide. Multiple factors in the water column and the surrounding biological community influence the dynamics of the coral microbiome. However, by including only temperature as an external factor, our model proved to be successful in describing the microbial community associated with the surface mucus layer (SML) of the coral *P. strigosa*. The dynamic model developed and validated in this study is a potential tool to predict the coral microbiome under different temperature conditions.

KEYWORDS host-microbe, metagenomics, microbial communities

The community structure of a host-associated microbiome is shaped by factors that are both extrinsic (e.g., abiotic conditions and community composition of micro- and macroorganisms in the surrounding environment) and intrinsic (e.g., microbial

Citation Lima LFO, Weissman M, Reed M, Papudeshi B, Alker AT, Morris MM, Edwards RA, de Putron SJ, Vaidya NK, Dinsdale EA. 2020. Modeling of the coral microbiome: the influence of temperature and microbial network. mBio 11:e02691-19. <https://doi.org/10.1128/mBio.02691-19>.

Invited Editor Monica Medina, Pennsylvania State University

Editor Margaret J. McFall-Ngai, University of Hawaii at Manoa

Copyright © 2020 Lima et al. This is an open-access article distributed under the terms of the [Creative Commons Attribution 4.0 International license](https://creativecommons.org/licenses/by/4.0/).

Address correspondence to Elizabeth A. Dinsdale, edinsdale@sdsu.edu.

* Present address: Maya Weissman, Department of Ecology and Evolutionary Biology, Brown University, Providence, Rhode Island, USA; Megan M. Morris, Department of Biology, Stanford University, Stanford, California, USA.

Received 8 October 2019

Accepted 14 January 2020

Published 3 March 2020

interactions and host physiology) to the holobiont (1–4). Identifying the role that each factor plays in predicting the diversity and community structure in the microbiome of host organisms is a major priority in microbial ecology, especially in the context of environmental changes (5–8).

Coral reefs are among the most productive, biodiverse, and endangered ecosystems in the world (9, 10), and the health of the reefs is directly mediated by the associated microbiota (11–14). Corals host one of the most phylogenetically diverse microbiomes among animal hosts (15), which is composed by endosymbiotic dinoflagellates (*Symbiodiniaceae*), bacteria, archaea, fungi, and viruses (16). The coral microbiome provides essential services to the holobiont, such as nutrient cycling (17–20) and protection against opportunistic pathogens via competition and the production of antibiotic compounds (21–23).

The symbiotic relationships in the coral holobiont are sensitive to changes in environmental conditions. Extrinsic factors, including eutrophication (24, 25), salinity (26), pH (27, 28), neighboring macroorganisms (4), herbivorous fish abundance (29), copper concentration (30), and temperature (27, 31–33), alter the taxonomic and functional composition of the coral microbiome. Overall, the response of the coral microbiome to environmental disturbances is consistent across multiple stressors, characterized by an increase in the relative abundances of *Vibrionales*, *Flavobacteriales*, *Rhodobacterales*, and *Alteromonadales* (33).

Corals are widely recognized as thermally sensitive organisms (34–37), and elevated temperatures are correlated with coral bleaching (i.e., loss of the algal symbiont) and disease outbreaks in coral reefs worldwide (32, 38–42). High seawater temperature causes the greatest change in the functional metabolism of coral microbiome, compared to eutrophication and low pH, as a result of an increase in the abundance of *Vibrio* spp. and other diseased-associated microbes (27). Seawater temperature, therefore, is one of the most important drivers of the coral-microbial community composition (43).

The surface mucus layer (SML) microbiome constitutes the direct interface between the coral host and the environment. Within the coral holobiont, the coral SML, tissue, and skeleton provide different microhabitats to the microbial community (44, 45). Across the three coral microhabitats, the microbial composition of the SML is the compartment that is most influenced by environmental factors (e.g., temperature, benthic coverage, and geographic region) (44) and by the microbial community in the water column (e.g., high similarity) (45).

The influence of factors that are intrinsic to the coral holobiont on regulating the microbiome is less clear. Host genotype and *Symbiodiniaceae* phylotype are among intrinsic factors that do not correlate with the taxonomic composition in the coral microbiome, but instead the microbiome correlates with environmental factors such as habitat and seasonality (46–48). Microbe-microbe interactions (e.g., competition, predation, mutualism), however, are intrinsic factors that are potentially major drivers of the coral microbial community structure and holobiont homeostasis (20, 49–52). Coral-associated bacteria produce inhibitory compounds and have antagonist effects on each other, including *Pseudoalteromonas* spp. inhibiting the coral pathogen *Vibrio shiloi* (51). High temperatures, however, can change the way microbes interact (53, 54). The number of coral-bacterial isolates inhibited by Alphaproteobacteria is drastically reduced when temperature increases from 25 to 31°C (51). Therefore, temperature and microbial interactions are interconnected and act simultaneously in shaping the community structure of the coral microbiome.

Mathematical models that use microbial growth rates as a function of environmental temperature (55–59) and include microbial interactions derived from network analysis (60, 61) can be a powerful tool to investigate the dynamics of microbial communities. However, this approach remains to be further adapted and applied to coral reef systems. The ecological interactions between the members of the microbiome are challenging to elucidate, but metagenomic sequencing (62–64), combined with network analysis, has been able to reveal these relationships (65–69). Microbial networks

A) Outer Reef Zone - OR



B) Inner Reef Zone - IR

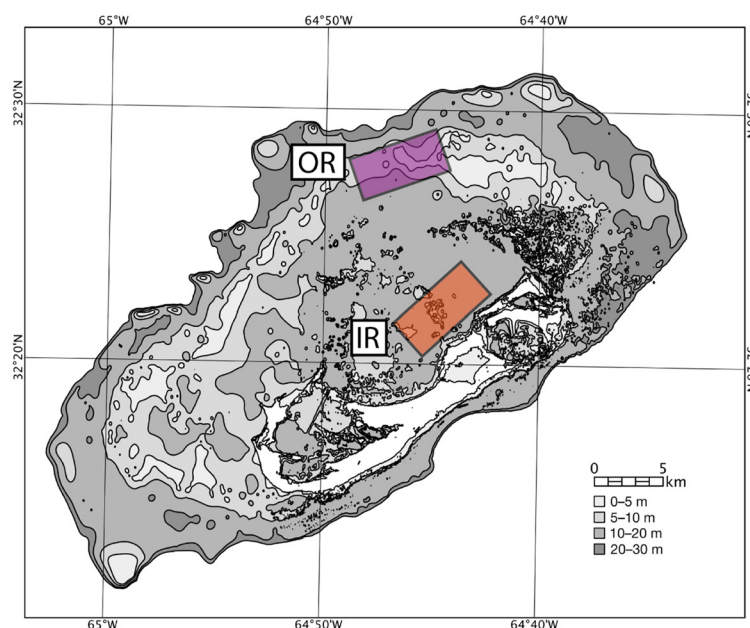


FIG 1 The coral reef in the Bermuda archipelago is composed of different reef zones across the platform. The outer rim reef (OR) is a relatively more stable thermal environment compared to the inner lagoon patch reefs (IR). Each reef zone was replicated ($n = 6$ corals per zone) in the colored areas.

constructed by correlation-based methods identify microbial interactions and the key taxa to the structure of the community by using measures of network centrality, such as eigenvector and betweenness centrality (70, 71).

Here, we develop a new differential equation mathematical model to determine the community structure of the microbiome associated with coral SML using temperature as an extrinsic factor and microbial network as an intrinsic factor to the coral holobiont. To provide the input data for the model development and validation, we selected the coral reefs of Bermuda, where coral colonies are exposed to different thermal regimes at a reef scale. The reef system in Bermuda is formed by distinct physiographic reef zones, and there is a pronounced spatial gradient in temperature profiles across the inner and outer reef zones. The seawater temperature differences of the shallow inner lagoon reefs range between 13 and 15°C (winter averages of 16 to 17°C and summer averages of 30 to 31°C), whereas the outer reef temperature range is moderated with a 10°C temperature difference (seasonal averages of 19 and 29°C, respectively) (72). The temperature profiles specific to each reef zone were simulated in the model. Metagenomic analysis was used to describe the taxonomic composition and generate the microbial network of the SML microbiome associated with the coral *Pseudodiploria strigosa* (Dana, 1846) from inner and outer reefs. The model was validated by comparing the predicted relative abundances of each microbial class to the measured relative abundances of each microbial class. Finally, the model was applied to six scenarios that combine different profiles of temperature and microbial network to investigate the drivers of the coral-microbial community dynamics. Our study shows that the SML microbiome of *P. strigosa* in Bermuda is primarily structured by reef-scale seasonal fluctuations in temperature, while the microbial network is a secondary driver.

RESULTS

Microbial community in the coral SML. The structure of the SML microbiome of *P. strigosa* was specific to each reef zone (Fig. 1) in terms of the relative abundances and microbial network parameters. The SML microbiome of *P. strigosa* included 30 bacterial and archaeal classes (inner reefs = 23, outer reefs = 21), with high proportional abun-

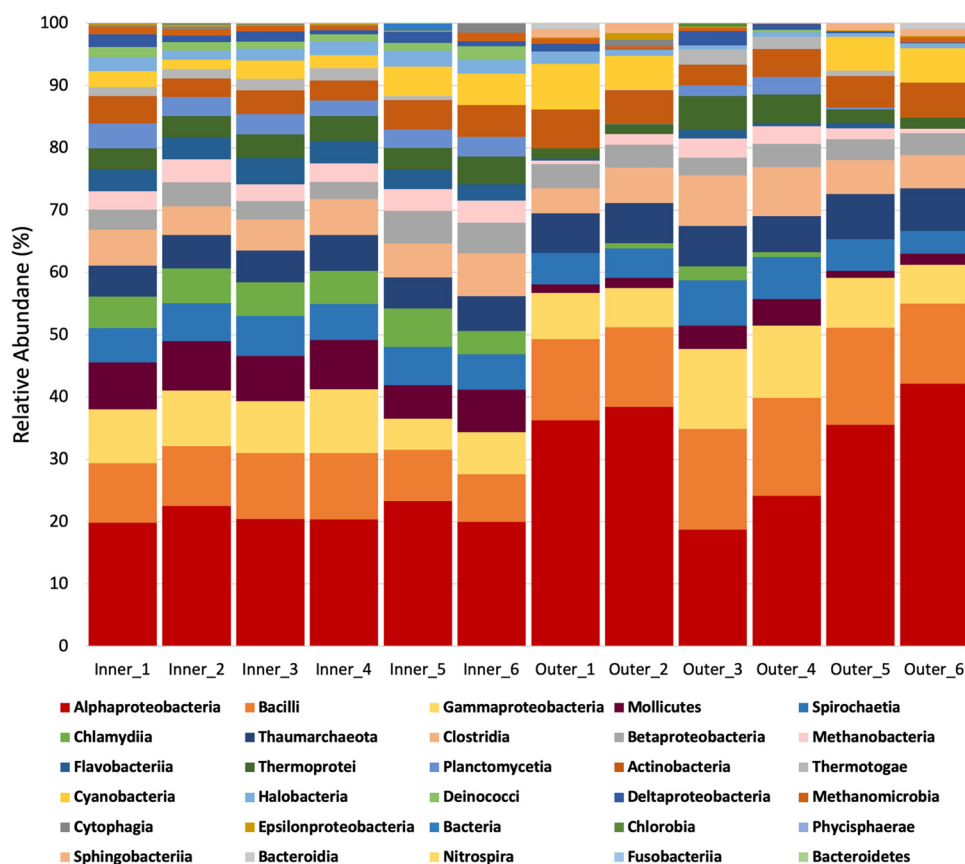


FIG 2 Relative abundances of microbial classes associated with coral SML from inner and outer reefs.

dances of *Alphaproteobacteria*, *Bacilli*, and *Gammaproteobacteria* (Fig. 2). Inner and outer reef microbial communities shared the same codominant classes, but the relative abundances of taxa were significantly different between reef types (PERMANOVA, Pseudo-F = 7.79; P(perm) = 0.004; see Table S1 in the supplemental material). The sample metagenomes from inner and outer reefs formed separate clusters, indicating that *P. strigosa* harbors a reef zone-specific SML microbiome (Fig. 3). There was lower intercolony variability in the SML microbial community within the inner reef corals compared to the outer reef corals (SIMPER, average similarity, inner = 92.9%, outer = 84.7%, see Table S2a and b). Therefore, the coral SML microbiome structure is more homogenous across host individuals of the same species in a more fluctuating environment than in a more stable environment in Bermuda. The inner and outer

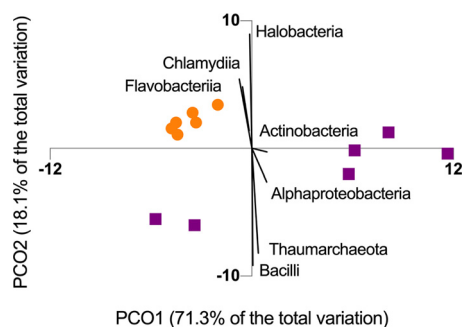


FIG 3 The SML microbiome of *P. strigosa* corals from the inner reefs (circles) showed greater clustering than corals from the outer reef (squares), visualized using a principal coordinate analysis of relative abundance of microbial classes. Vectors correspond to Spearman's correlation indices higher than 0.9.

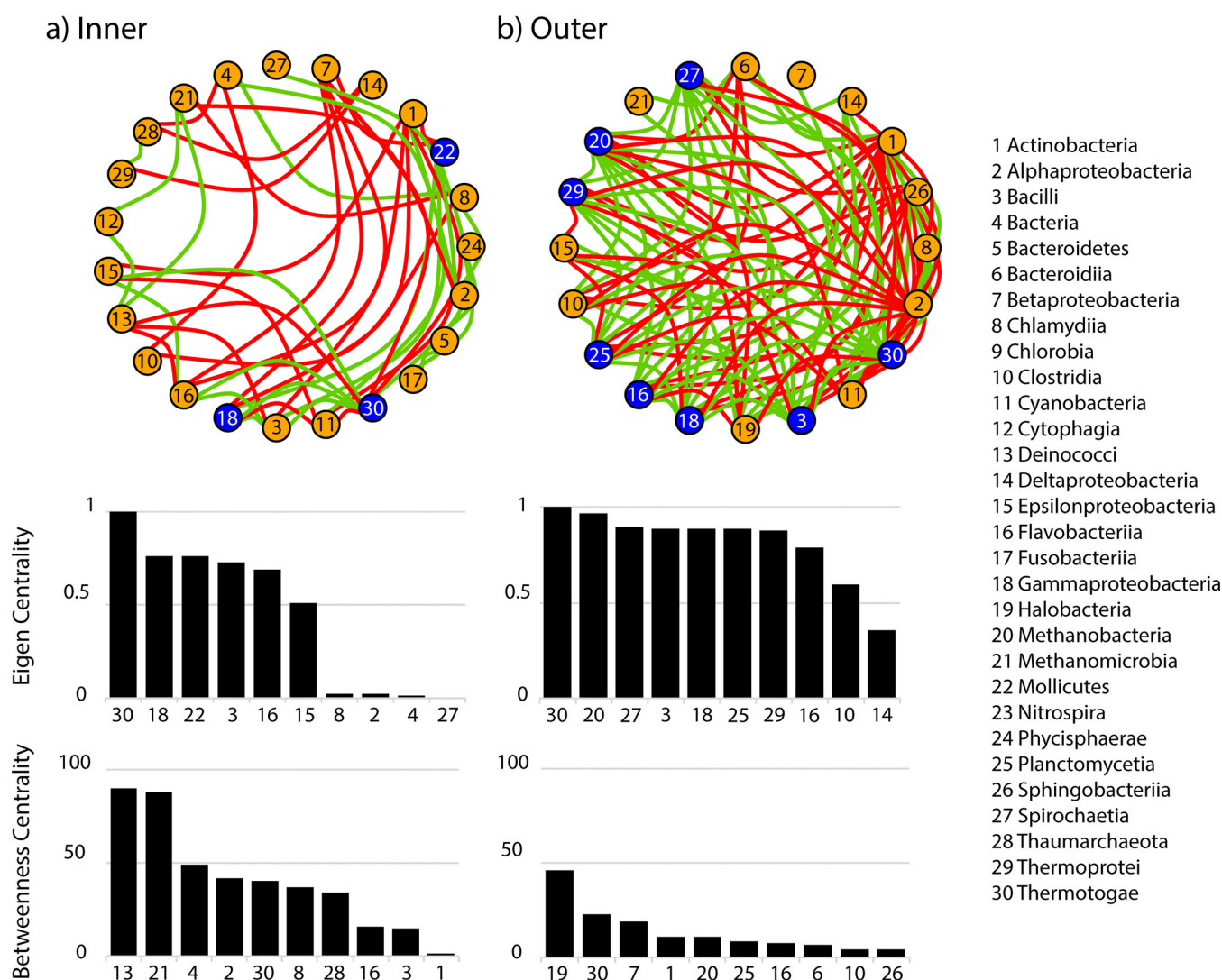


FIG 4 Network analysis of the coral SML microbiome of *P. strigosa* from inner (A) and outer (B) reefs. Each node represents a microbial class interconnected by positive correlations (green) and negative correlations (red) (Spearman's $\rho > 0.7$). Nodes that have an eigen centrality higher than 0.75 are highlighted in blue. The top 10 values of eigen centrality and betweenness centrality across microbial classes are graphed below each network.

coral-mucus microbiome had an average dissimilarity of 18.16% (Table S2c). The main classes contributing to the dissimilarity between reef zones were *Chlamydia*, *Deinococci*, and *Flavobacteriia*, which were overrepresented in the microbiome of corals from inner reefs.

The SML microbiome from each reef zone showed a specific network (Fig. 4). The microbial network from inner reefs had 23 nodes (i.e., microbial classes), 46 edges, and a diameter of 7, while the microbial network from outer reefs had 20 nodes, 94 edges, and a diameter of 3. The network in the outer coral SML microbiome was more tightly connected compared to the inner coral SML microbiome taxa (eigen centrality > 0.75 , $n = 8$ classes in outer reefs and $n = 3$ classes in inner reefs; Fig. 4). High values of eigen centrality characterize a highly structured community network, in which the relative abundances of microbial taxa are tightly correlated (73). On the other hand, the microbial network from inner reefs showed higher betweenness centrality and lower eigen centrality (maximum betweenness = 45 in outer reefs and 90 in inner reefs; Fig. 4). A microbial class with a high level of betweenness centrality sits at a position that is important in facilitating the connectivity of the network (74). *Thermotogae*, even though it was a rare class (average relative abundance of $< 1\%$) showed high eigen and

TABLE 1 Model scenarios generated by different combinations of network parameters and temperature profiles

Model Scenario	Network Parameters		Temperature Profiles		
	Specific	Generalized	Specific, fluctuating	Generalized, fluctuating	Constant
SN-ST					
SN-GT					
SN-CT					
GN-ST					
GN-GT					
GN-CT					

betweenness in both reefs. *Methanobacteria* is a key node to the network of coral microbiome in outer reefs, with both high eigen centrality and betweenness centrality (Fig. 4). In the microbiome of corals from inner reefs, *Gammaproteobacteria*, *Mollicutes*, *Bacilli*, and *Flavobacteriia* showed the highest eigen centrality, and *Deinococci*, *Methanomicrobia*, and *Alphaproteobacteria* showed the highest betweenness centrality in the community network (Fig. 4).

Modeling the coral microbiome. We developed a dynamic model based on differential equations to describe the relative abundances in the microbial community associated with the coral mucus in response to temperature and microbial network. The model uses classical logistic growth equations to calculate growth rates for each microbial class as a function of seawater temperature over time (59) and accounts for the effects of microbial interactions on growth rates using network correlation coefficients (60). The model was validated by comparing model prediction with sample data, using the classes identified in the metagenomes that showed an average relative abundance greater than 1% in at least one of the two reef zones ($n = 17$ classes shared between reef zones, out of the total of 23 in the inner reefs and 21 in the outer reefs). For both the inner and outer reefs, we used the corresponding specific networks and corresponding temperature profiles into the model of the SML microbiome of *P. strigosa* and solved the model to predict the microbiome composition (Fig. S1). Linear regression of the sample data and the model prediction of abundance of each microbial class had a slope of 0.96 and an intercept of 0.45, which were not statistically significant different from one and zero, respectively (Wald linear hypothesis test, sum of squares = 8.52, $F = 0.81$, $P = 0.55$). Therefore, the mathematical model developed in this study was accurate in predicting the observed SML microbiome of *P. strigosa* from the sample data, and the approach implemented here is appropriate for modeling the coral microbiome.

Investigating the role of temperature and microbial network as model components for the coral microbiome. We used our model to determine the key drivers governing the community structure in the coral SML microbiome. Six different combinations of temperature profiles (T = fluctuating temperature; CT = constant temperature) and network structures (N) that were both either specific to the reef zone (S) or generalized to the coral reef system (G) were evaluated (Table 1). An example scenario is SN-ST, which combines specific network and specific fluctuating temperature. The same model scenarios were applied to the microbiome associated with each reef zone (inner and outer reefs) separately generating twelve corresponding model outputs total (Fig. 5). Ten of the total of twelve model outputs analyzed had a significant linear regression between sample data and model predictions (Fig. 5a to d and g to l). Model outputs that significantly described the relative abundances of sample data produced R^2 values ranging from 0.51 to 0.70 (Table S3). Model scenarios that used constant

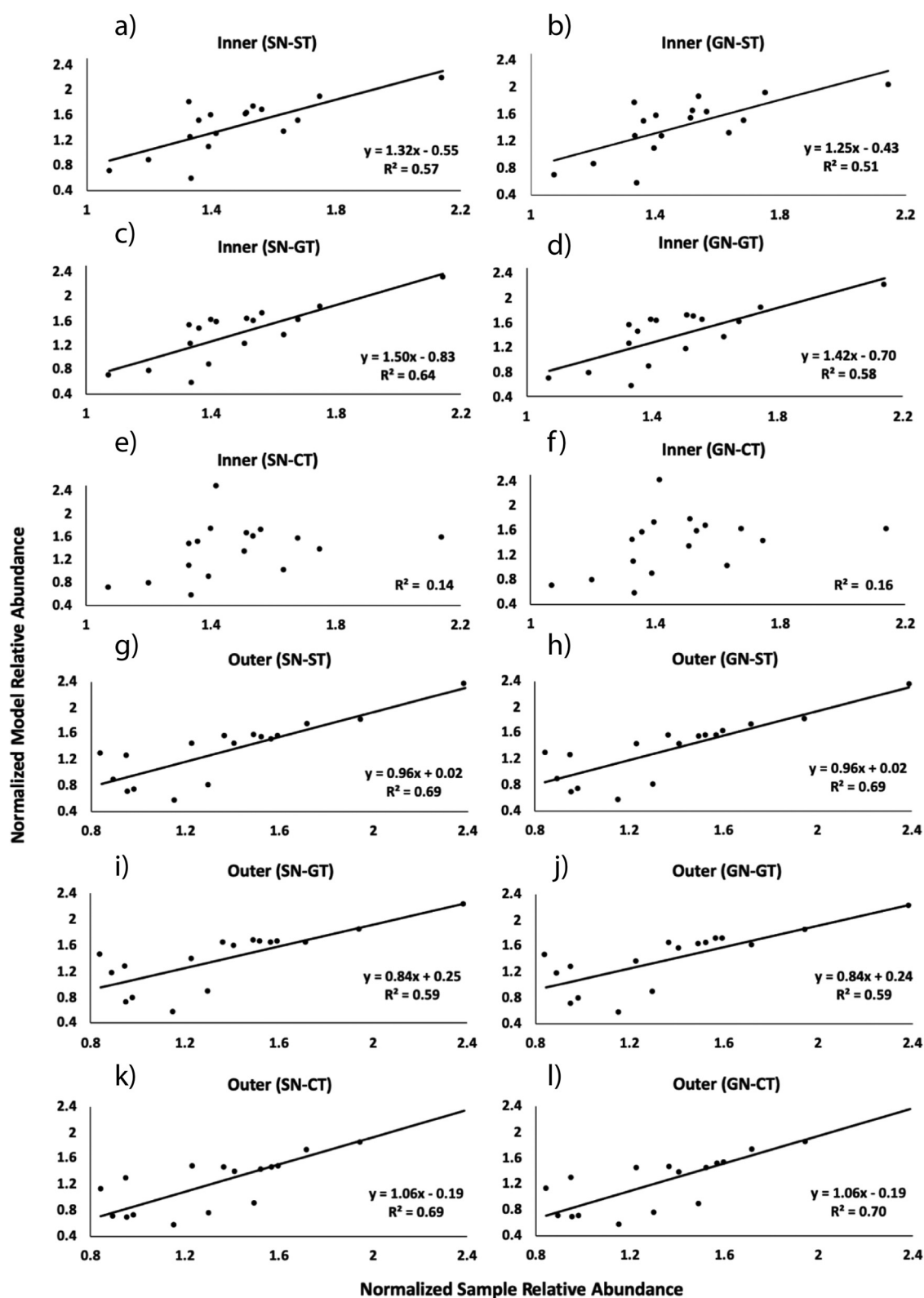


FIG 5 Linear regression analysis between sample and model data based on fourth-root transformed relative abundances. The sample data corresponds to the most abundant microbial classes ($n = 17$, average abundance $>1\%$) in the metagenomes sequenced from surface mucus layer of the coral *P. strigosa* ($n = 12$ colonies; 6 per reef zone). The model abundances of these same classes were generated by the mathematical model for both inner (a to f) and outer reefs (g to l) using six different scenarios. The solid lines represent significant linear regressions (ANOVA, $P < 0.05$).

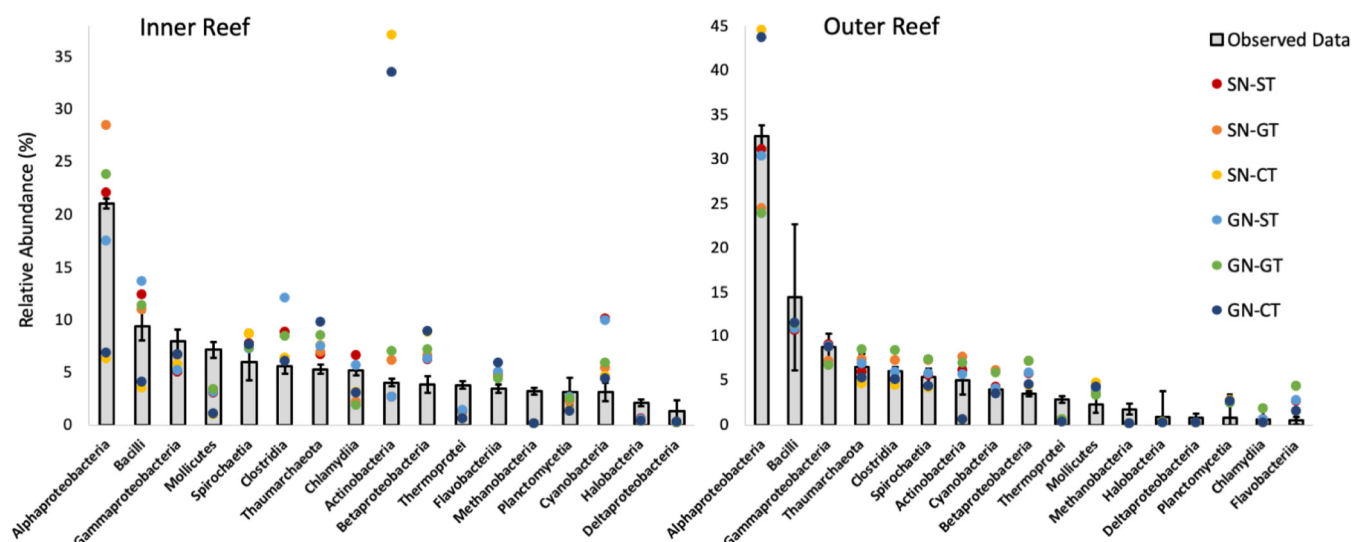


FIG 6 Model predictions of the relative abundances of seventeen microbial classes generated using the six scenarios (SN-ST, SN-GT, SN-CT, GN-ST, GN-GT, and GN-CT) compared to the observed data (means \pm the standard deviations; $n = 6$ per reef zone) for the inner and outer reef zones, respectively.

temperature profiles were not significantly correlated with the coral microbiome from inner reefs (Fig. 5e to f, inner SN-CT, GN-CT, $R^2 = 0.1$). Therefore, the coral SML microbiome from inner reefs could not be successfully predicted by our model under constant temperatures, regardless of the network used. In contrast, when the temperature was kept constant in outer reefs, the model output accurately described the measured microbiome.

Among the ten model scenarios that fit the linear regression analysis, some combinations of microbial network and seawater temperature profiles generated more accurate outputs (higher R^2) than others. In inner reefs, the greatest accuracy is achieved by using a specific network and an average fluctuating temperature profile (Fig. 5c, inner SN-GT, $R^2 = 0.64$). The accuracy of the model output is lower when a generalized network and a warmer and more fluctuating temperature profile is applied (Fig. 5b, inner GN-ST, $R^2 = 0.51$). The microbiome of corals from the outer reefs of Bermuda was best predicted by the model compared to inner reefs since all model scenarios produced significant linear regressions. The outputs produced by the model scenarios that used milder fluctuating temperature profiles (Fig. 5g and h, outer SN-ST, GN-ST) and constant temperature profiles (Fig. 5k and l, outer SN-CT, GN-CT) showed similar accuracies ($R^2 = 0.69$), regardless of the network profile. Model scenarios that used an average fluctuating temperature profile (Fig. 5i and j, outer SN-GT, GN-GT) generated outputs with lower accuracy ($R^2 = 0.59$) in outer reefs.

The accuracy of the model relative abundances in the coral SML microbiome varied across taxa between the two reef zones (Fig. 6). *Alphaproteobacteria*, the most proportionally abundant taxon in the coral SML microbiomes of both reef zones, was more accurately predicted by model scenarios that used reef-specific temperature profiles (Fig. 6, SN-ST, GN-ST). On the other hand, model scenarios that used constant temperature profiles (Fig. 6, Inner SN-CT, GN-CT) were the least accurate when modeling the abundance of *Alphaproteobacteria*, causing underestimation in inner reefs and overestimation in outer reefs. Other codominant taxa, such as *Bacilli* and *Mollicutes*, were also underrepresented in the “CT” model scenarios in inner reefs. *Actinobacteria* was overestimated by approximately 8-fold under constant temperatures in inner reefs (Fig. 6, inner SN-CT, GN-CT). The model scenarios applied to the coral SML microbiome of outer reefs produced outputs that were within the range of the standard deviation from the mean relative abundances of the observed data for most of the microbial classes (Fig. 6).

Mathematical modeling of the coral SML microbiome

A) Model application work flow:

$$\frac{dB_i}{dt} = R_i(T(t)) \cdot B_i \cdot \left(1 - \frac{\sum_{j=1}^n B_j}{k}\right) \cdot \left(1 + \sum_{j=1}^n \eta_{ij} \cdot B_j\right)$$

- 1) Select the **source environment** based on local seawater annual temperature regime ($T(t)$)
- 2) Sample the **surface mucus layer (SML)** of multiple **individuals** of the target species from the selected environment
- 3) Sequence and **analyze metagenomes** to decide which taxa to model (B) and the network parameters (η) to apply
- 4) Compile **literature data on growth rates** of the selected microbial taxa and calculate R
- 5) Run the **model** and compare the observed and the model data.
- 6) Explore **different scenarios of temperature and network profiles** and their effect on the coral-microbial community

B) Model system: the SML microbiome of *P. strigosa* across reef zones in Bermuda

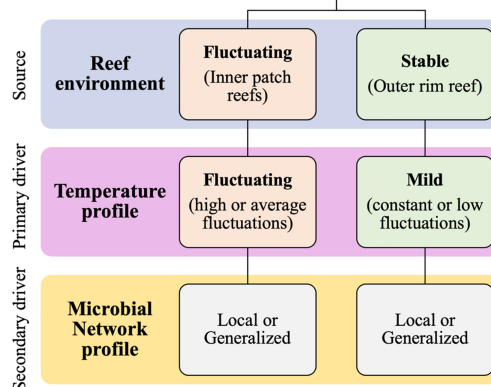


FIG 7 Modeling the coral surface mucus layer (SML) microbiome. (Left) Suggested workflow to apply the model developed in this study. (Right) Conceptual schematic of the drivers of the microbial community structure within the mucus of *P. strigosa* from each reef environment in Bermuda. The seawater temperature profile is the primary driver predicting the coral microbiome structure associated with different reef zones. Greater accuracy between the model and sample data were achieved when the model temperature profile depicts the natural temperature regimes. The network profile, used as a proxy for the microbial community interactions, is considered a secondary driver since it did not influence the accuracy of the model scenarios.

DISCUSSION

The mathematical model we developed predicted the microbial relative abundances in the SML microbiome of the coral *P. strigosa* and is a robust tool for investigating the effects of different profiles of temperature and microbial network on the model microbiome. We considered temperature as the major driver affecting the predictability of the coral SML microbiome of both reef zones compared to microbial network (Fig. 7). Differences in accuracies were driven by the distinct temperature profiles used across the model scenarios, while different microbial network profiles caused no apparent effect. The SML microbiome was best predicted by model scenarios that had a temperature profile that is closest to the local thermal environment. The coral SML microbiome in inner reefs in Bermuda is more exposed to natural temperature fluctuations (72, 75, 76). Therefore, a fluctuating profile is crucial to accurately describe the microbiome from that reef zone using temperature as an extrinsic factor. The coral SML microbiome of inner reefs is best predicted by the model scenarios that include high (SN-ST; GN-ST) or average (SN-GT; GN-GT) temperature fluctuations, since there is a significant loss in model fit when the temperature is kept constant (SN-CT; GN-CT), regardless of the associated network. In contrast, the SML microbiome of corals in the outer reefs were modeled using any temperature or network profile but the model outputs were less accurate when a warmer and more fluctuating temperature profile was applied.

The model shows that the coral SML microbiome from a fluctuating environment is more sensitive to the temperature profile used to achieve accurate predictions of the microbial relative abundances. This indicates that temperature is exerting a stronger and more directional pressure on the microbiome of inner reef corals, as they experience more pronounced temperature fluctuations than corals from the outer reefs (annual temperature range of 13 to 15°C in inner patch reefs and 10°C in outer reefs) (72). The sample data show that the coral SML microbiome structure is more homogenous across host individuals of *P. strigosa* in inner reefs than in outer reefs. Stability in the microbiome among colonies exposed to environmental stress is characteristic of a directional, rather than stochastic, response to pressure (77). Microbiome stability under

environmental fluctuations was an unexpected finding. Previously, the microbiome of *P. strigosa* showed high variability under stress conditions *in situ*, compared to *Diploria labyrinthiformis*, a closely related species (78). However, the microbiome of *P. strigosa* shows low intercolony variation within the same site over time in the Caribbean (79), indicating that the microbiome associated with different colonies of *P. strigosa* acclimates similarly to temporal variability, which could explain the stability among inner reef corals. The local temperature profile may also influence the differences in the relative abundances between the microbiomes from inner and outer reefs. *Chlamydia* and *Flavobacteriia* are driving the difference in the microbiomes between the two reef zones. The abundance of *Flavobacteriia* increased in the microbiome of *P. strigosa* in the summer compared to winter (78) and both taxa have been associated with elevated temperatures in coral reef environments (27, 33, 80–82). The overrepresentation of members of these classes in the microbiomes of corals from inner reefs of Bermuda may be related to the warmer local temperature profile but can also be simultaneously influenced by other factors (e.g., fluctuations in dissolved organic carbon [DOC]) (83, 84). The coral holobiont responds to fluctuations in abiotic factors such as light availability, pCO₂, total alkalinity, pH, dissolved inorganic carbon (DIC) (76), and DOC (12, 14, 85). These could also be driving the community structure in the SML microbiome of corals and be potential extrinsic factors to be added to our model. However, in Bermuda, many of these variables are correlated with seasonal temperature fluctuations (76), which could partially explain why seawater temperature as the only abiotic factor is sufficient to accurately model the SML microbiome of corals.

The specificities of the microbial networks associated with each reef zone are also in accordance with trends shown in the model and the microbial community composition. Cooccurrence networks are able to detect small-scale environmental differences and show network specificity to each environment (86). The coral SML microbiome from outer reefs was more variable between individual corals, but the microbial network was highly structured, because many microbial classes had high eigen centrality, whereas betweenness centrality across taxa was low. High eigen centrality and low betweenness centrality are characteristic of keystone taxa in microbial networks (86). The milder environment in outer reefs could be releasing the coral SML microbiome from constant microbial community turnover caused by external disturbances, allowing the microbial community to establish several different cooccurrence patterns and generating more hubs of keystone taxa in the network, e.g., in the microbial network of outer reefs eight classes had an eigen centrality of >0.75 compared to three classes in the network of inner reefs. A host-associated microbial network that is less disturbed is characterized by nodes that are more interdependent and is more vulnerable to targeted disturbances, since the removal of hub species caused a greater disruption of the network diameter (87). The microbial network associated with the SML microbiome of inner reef corals showed the opposite structure, composed of high values of betweenness centrality and low eigen centrality. Host-associated microbial networks characterized by high betweenness centrality and low occurrence of large hubs of interconnected microbial taxa are considered resilient because the removal of nodes would not greatly impact the connectivity of the others (88). Therefore, the coral SML microbiome in the inner reef zone in Bermuda is organized in a network structure that potentially confers resilience to the microbial community exposed to environmental disturbances, while the outer reefs provide a more stable environment that is conducive to a tightly connected microbial network.

Coral reefs provide a variety of habitats characterized by different environmental conditions, which affect the biological community from the scale of macro- to micro-organisms (4, 12, 89, 90). Our results are in agreement with studies that show that the reef zone in which the coral colony resides is a major factor shaping the coral microbiome composition (46, 48), particularly across areas exposed to different thermal regimes (47). The spatial gradient in temperature profiles across the reef zones in Bermuda is coupled with documented variations in coral growth, calcification (76), and

reproductive processes (75, 91, 92). We showed that the coral SML microbiome responds to the local thermal environment in the coral reefs of Bermuda.

Model applicability and future directions. Coral microbiome dysbiosis (i.e., shifts in the community structure or a complete loss of microbial symbionts) caused by changes in the environment is a key mechanism in the decrease of coral health worldwide (13, 29, 50, 93). The lack of data sets describing long-term coral-microbe dynamics is interfering with successful predictions of how environmental change will affect the coral holobiont (43). Metagenomics followed by modeling and prediction are highlighted as main analytical tools to disentangle coral disease causation and to identify the successful application of mitigation strategies (94). The dynamic model we developed and validated using sampled metagenomes has the potential to be applied in microbial ecology research and coral reef management. A caveat to this study is that only one time point was used to validate the dynamic model. A time series of the coral microbiome *in situ* will further improve the model with regard to the temporal fluctuations in the microbiome structure. However, the model produced accurate outcomes across multiple scenarios of temperature and network profiles, suggesting that the model is very robust. We modeled the coral SML microbiome at the class level to obtain a number of taxa that are large enough to be representative of both two reef zones and achieve model accuracy, since all of the differential equations for each taxon are solved simultaneously. After the rare taxa (relative abundance < 1%) were removed, we had more than 70% of the total richness identified in the metagenomes represented in our model. We note that our model can be implemented using other taxonomic levels (e.g., order, family, and genera), if the parameters that are necessary to calculate growth rates $R(T)$ are known for each taxon. We recommend the use of a cutoff value to remove the rare taxa and maintain the accuracy of the predicted relative abundances.

The model is relatively simple to use and to interpret and can be used to simulate the changes in the SML microbiome in response to seasonal temperature fluctuations (Fig. 7). Coral species exhibit a wide variation in thermal resilience (95–97) and mucus production and composition (98), which indirectly shapes the associated SML microbiome. The coral *Porites astreoides*, for example, goes through cycles of mucus aging and shedding that affects the microbiome dynamics (99). Therefore, the model developed here could be used to identify whether the microbiomes of other species are affected by temperature like the *P. strigosa* SML microbiome. We recommend at least one annual collection of the mucus microbiome for metagenomic analysis across different reef environments for model calibration. This approach will allow for a level of resolution specific to different areas across the reef that might require distinct management decisions. For example, the model can be used to evaluate whether different environments across the reef are more susceptible to disease or dysbiosis due to a predicted change in the relative abundances of microbial taxa under specific temperature conditions. Our model can also be used to describe the microbiome associated with the coral tissue and skeleton following the same workflow that we developed for the SML microbiome (Fig. 7). However, since each compartment provides a specific microhabitat to the microbial community (44, 45), the coral tissue and skeleton microbiomes may respond differently to temperature fluctuations compared to the SML microbiome (44). We encourage the application of this model to other compartments of the coral microbiome (i.e., tissue and skeleton), as well as different coral species and coral reef systems, to compare whether temperature remains the primary ecological driver of the host-associated microbiome compared to the microbial network.

MATERIALS AND METHODS

***In situ* collections.** The mucus from *P. strigosa* was collected from six colonies from the inner and outer reef zones ($n = 12$ colonies total) in May and June 2017. Each reef zone was replicated across three reef sites (Fig. 1). The SML microbiome of *P. strigosa* colonies (diameter, 10 to 15 cm) was collected using a “supersucker,” a two-way 50-ml syringe filled with 0.02- μ m-filtered seawater (100). The filtered seawater is flushed across the coral surface, dislodging the mucus and associated microbes, which are

then sucked up via the recirculating tube, and the resulting sample pushed through a 0.22- μ m Sterivex (EMD Millipore) for DNA extraction. We collected 200 ml of coral mucus diluted in sterile seawater (four supersuckers) per colony to increase DNA concentration per sample. The reef water microbiome was also analyzed to control for contamination in the mucus samples (results not shown). The collections were performed via SCUBA diving at a depth of 4 to 6 m.

Metagenomics analysis. Microbial DNA from the coral mucus was extracted using a modified Macherey-Nagel protocol from 0.22- μ m Sterivex using NucleoSpin column for purification. DNA was stored at -20°C until quantification with Qubit (Thermo Fisher Scientific) (14). The Swift kit 2S plus (Swift Biosciences) was used for library preparation since it provides good results from small amounts of input DNA, characteristic of microbial samples collected from the surface of the host (100–102). All samples were sequenced by the Dinsdale lab on Illumina MiSeq at San Diego State University (103). The Illumina MiSeq is one of the best sequencing technologies for short genomes, such as those associated with bacteria and archaea, and provides longer reads compared to the Illumina HiSeq (104, 105). We described the proportional abundance of *Bacteria* and *Archaea* in the coral mucus microbiome using shotgun metagenomics (62, 64). The sequenced DNA was analyzed for quality control using PrinSeq (106) before annotation. The forward and reverse reads were paired using PEAR (107). The sequencing depth ranged from 582,582 to 1,256,934 reads per metagenome (see Table S4 in the supplemental material). FOCUS (108), which is a K-mer-based approach, was used to annotate taxa. FOCUS has been identified as one of the top profiling analysis tools by CAMI (109). The number of sequence hits for each microbial taxon is represented as the relative abundance by calculating the proportion of sequence hits for that class over the total number of sequences annotated for that metagenome.

Statistical analysis of the sample data. Statistical analyses were conducted using PRIMER v7 plus PERMANOVA and R (R Project for Statistical Computing). Significant differences in the relative abundances of classes in the coral microbial communities sampled from inner and outer reefs were identified by permutational multivariate analysis of variance (PERMANOVA) using Bray-Curtis distances of normalized relative abundance obtained using a fourth-root transformation. A principal coordinate analysis was created to visualize the separation of the coral microbiome between inner and outer reefs and the most important taxa driving the cluster by plotting the vectors corresponding to Spearman's correlation indices. A SIMPER analysis was performed to identify the taxa responsible for the similarity of the microbiomes within reef zones and dissimilarity between reef zones. The microbial network was constructed for each metagenomic data set the taxonomic pairwise Spearman correlation matrix calculated in R. The matrix was calculated for each reef zone, and the network correlation coefficients were used in the dynamic model described in under "Mathematical model" below. The Python packages pandas (110) and networkx (111) were used to test for subclustering of the networks and identified that each network remains a single connected component. The R package igraph (112) was used to construct a network using the microbial taxa at class level as nodes and the Spearman correlation values as edge weights. The calculated diameter of the network was unweighted. Taxonomic cooccurrences that met or exceeded the preset correlation threshold were kept, while all other values were transformed to 0. The psych package (113) was used to calculate the *P* value for all pairwise coefficients. All pairwise coefficients from which the *P* value exceeded 0.001 were discarded from the analysis. To identify taxa that occupy important structures of the microbial network, the R package igraph was used to calculate the eigenvector and betweenness centrality. Eigen centrality identifies highly connected nodes that are connected to other highly connected nodes (114, 115). Betweenness centrality calculates the shortest path through a network and keeps record of how many times a node in a network is traversed (74). If a node is traversed frequently, the node in the network is considered to sit at a position that is important in facilitating the connectivity of the network. If the taxon has a high betweenness centrality, then it sits at a position in the network that is responsible for facilitating correlations between different taxa. Without the presence of that taxon, the network loses the architecture that binds it together in an ordered way.

Mathematical model. In an isolated environment, we assume that each microbial class, B_i , grows according to the classical logistic growth equations; however, growth rate, $R_i(T(t))$, is represented as a function of the environmental temperature, $T(t)$, which changes over time. Since each microorganism has a distinct range of ideal temperatures for its growth, we consider the growth rate, $R_i(T(t))$, to be normally distributed with mean at the midpoint of the range of the ideal temperature as follows.

$$R(T) = R_{\max} \cdot \frac{1}{\sqrt{2\pi\sigma^2}} \cdot e^{-\frac{(T-\mu)^2}{2\sigma^2}}$$

Here, R_{\max} is the maximum growth rate, μ is the mean ideal growth temperature, and σ is the range of ideal temperatures. These values are specific to each microbial taxon and are summarized in the Table S5 in the supplemental material. The values used in the calculation of maximum growth rates were obtained from the literature for cultured representatives of each microbial class.

Variation in temperature is captured using a sinusoidal function (59),

$$T(t) = M + A \cdot \sin(\omega \cdot t + \theta),$$

where M and A represent the mean and the amplitude of the temperature profile. ω is related to the period of the periodic temperature profile, i.e., the period is $2\pi/\omega$ and θ represents the phase shift of the temperature used to make the temperature equation more accurately reflect the temperature conditions in the reefs of Bermuda according to the literature (72, 75, 76). The differences in reef zone environment are represented with different values for M and A , as described under "Network and temperature profiles" below.

When the microorganisms reside in a community together, such as in the coral mucus, there are two major potential effects each microbial taxon faces due to the presence of one another: (i) all microbes compete for the common resources denoted by the total carrying capacity (k), and (ii) interactions among microbes in a network alter the net growth rate of each other. To introduce the first effect into the model, we assumed that all taxa compete identically for the common resources since their relative competition coefficients are not well established. The second effect is introduced by altering the net growth rate of each microbial taxon with all other components of the microbiome according to its network correlation coefficients. The model we use is as follows:

$$\frac{dB_i}{dt} = R_i(T(t)) \cdot B_i \cdot \left(1 - \frac{\sum_{j=1}^N B_j}{k}\right) \cdot \left(1 + \sum_{j=1}^N \eta_{ij} \cdot B_j\right), i = 1, 2, \dots, N.$$

Here, N is the total number of taxa, k represents the carrying capacity, and η_{ij} represents the network correlation coefficient between the i th class and the j th class of bacteria.

Network and temperature profiles. The model uses network correlation coefficients [η_{ij} and temperature fluctuations over time $T(t)$] to predict the structure of the microbial community associated with coral mucus. Therefore, different profiles of microbial network and seawater temperature were selected in an ecological context of the coral reef system. For both network and temperature, we explored the specificities of each reef zone by including a “specific” profile. In addition, we also considered a “generalized” profile that represents the coral reef system on a broader scale, instead of according to the local zonation patterns. “Specific” and “generalized” profiles are used to evaluate whether the inclusion of values that represent the microbiome (network) and the environment (temperature) at a fine spatial scale are necessary to achieve accuracy in the model outputs.

The specific network profiles (SN) include the correlation coefficients (η_{ij}) that represent the sample data collected in the specific reef zone being modeled. For example, to model the microbiome associated with inner reefs, the correlation coefficient (η_{ij}) produced from all of the six metagenomes collected in inner reefs is used in the SN profile. In contrast, the generalized network profile (GN) uses the correlation coefficient (η_{ij}) produced by all the metagenomes collected from both reef zones ($n = 12$).

The specific temperature profiles (ST) are produced by using yearly mean (M) and amplitude (A) in degree Celsius that are representative of each reef zone to calculate the temperature fluctuations as a function of time $T(t)$. In the ST profile for the inner reef, the temperature mean and the amplitude are higher ($M = 24$, $A = 7$) than in the ST profile for the outer reef ($M = 18$, $A = 5$). Therefore, the ST profiles are developed to represent the local temperature regimes in terms of annual temperature fluctuations, in which the inner reef zone is a warmer and more fluctuating environment and the outer reef zone is a milder and more stable thermal environment. The generalized temperature profile (GT) used the average between the parameters in the ST profiles ($M = 21$, $A = 6$). In all of the temperature profiles, we used $\omega = 2\pi/365$ to account for the annual variability of temperature according to seasons (Fig. S2). Constant temperature profiles (CT) are also considered to evaluate the effect of temperature fluctuations on the model outputs. The CT profiles use the mean temperatures specific to each reef zone, (inner: $M = 24$, $A = 0$; outer: $M = 18$, $A = 0$).

Model application to identify drivers of microbiome dynamics. The mathematical model we developed considers both intrinsic and extrinsic factors affecting the coral mucus microbiome. The intrinsic factor is the microbial interaction within the microbiome, characterized by the network analysis, and the extrinsic factor is environmental temperature. To determine the key drivers governing coral mucus microbiome composition across reef zones, we evaluate six different model scenarios (i.e., different combination of network and temperature profiles):

- (i) Specific network, specific temperature (SN-ST): both the temperature profile and network parameters used are specific to each reef zone.
- (ii) Specific network, generalized temperature (SN-GT): the network profile is specific for each reef zone, but the temperature profile is generalized.
- (iii) Specific network, constant temperature (SN-CT): the network profile is specific to each reef zone, but temperature remains constant at the mean specified for each reef zone.
- (iv) Generalized network, specific temperature (GN-ST): the network profile is generalized, but the temperature profile is specific for each reef zone.
- (v) Generalized network, generalized temperature (GN-GT): the network profile and the temperature profile are generalized.
- (vi) Generalized network, constant temperature (GN-CT): the network profile is generalized, and the temperature remains constant at the mean specified for each reef zone.

Statistical analysis of the model output data. The microbial relative abundances generated from the model were compared to the sample data from inner and outer reefs using a linear regression (in R Project for Statistical Computing). A Wald linear hypothesis test was performed on the parameters generated by the linear regression analysis (i.e., slope and intercept). If the model is an accurate predictor of the coral microbiome, the slope will not be statistically different from 1, and the intercept will not be statistically different from 0. Each model scenario was tested by the fourth-root transformation of sample data, and model relative abundances were applied to achieve normality (Shapiro-Wilk test); a linear regression analysis was then performed and tested. Model components associated with changes in accuracy (R^2) of the model outputs are considered key factors shaping the coral microbiome structure. For example, if all model scenarios that include “ST” are more accurate than the others, regardless of the network profile used, then the local temperature profile is a key factor. Therefore, temperature is a primary driver, and microbial interactions is a secondary driver shaping the coral microbiome structure. If there are no differences in accuracies across model scenarios, then it is assumed that all factors have

the same impact on the microbial community. Therefore, by comparing the model outputs generated by different combinations of network and temperature profiles, the model was applied to investigate the drivers of the coral-microbial community dynamics.

Data availability. The metagenomic data from this study is publicly available in the SRA database as BioProject [PRJNA595374](https://www.ncbi.nlm.nih.gov/bioproject/595374) (<https://www.ncbi.nlm.nih.gov/bioproject/595374>) and in MG-RAST as public study SDSU_BIOS_2017 (mgp81589; <https://www.mg-rast.org/linkin.cgi?project=mgp81589>). The scripts used for the statistical analysis in R, Python, and PRIMER are publicly available as a GitHub repository under “MichealBReed/Microbiome_model” (https://github.com/MichealBReed/Microbiome_model).

SUPPLEMENTAL MATERIAL

Supplemental material is available online only.

FIG S1, TIF file, 2.2 MB.

FIG S2, TIF file, 2.5 MB.

TABLE S1, DOCX file, 0.01 MB.

TABLE S2, DOCX file, 0.02 MB.

TABLE S3, DOCX file, 0.01 MB.

TABLE S4, DOCX file, 0.01 MB.

TABLE S5, DOCX file, 0.01 MB.

ACKNOWLEDGMENTS

We thank San Diego State University (SDSU)/University of California, Davis (UCD), Joint Doctoral Program in Ecology at SDSU/UCD, SDSU Graduate Travel Awards, and the Bermuda Institute of Science (BIOS) Grant-in-Aid Sydney L. Wright and Wolfgang Sterrer Fellowships for supporting Ph.D. candidates L.F.O.L. and A.T.A. with travel costs and research expenses at BIOS. The work of principal investigator N.K.V. and undergraduate student M.W. on the model development was supported by National Science Foundation grants DMS-1616299 and DMS-1836647 and by a UGP award from SDSU. The funders had no role in study design, data collection and interpretation, or the decision to submit the work for publication.

REFERENCES

- Bordenstein SR, Theis KR. 2015. Host biology in light of the microbiome: ten principles of holobionts and hologenomes. *PLoS Biol* 13:e1002226. <https://doi.org/10.1371/journal.pbio.1002226>.
- Soen Y. 2014. Environmental disruption of host-microbe coadaptation as a potential driving force in evolution. *Front Genet* 5:168. <https://doi.org/10.3389/fgene.2014.00168>.
- Foster KR, Schluter J, Coyte KZ, Rakoff-Nahoum S. 2017. The evolution of the host microbiome as an ecosystem on a leash. *Nature* 548:43–51. <https://doi.org/10.1038/nature23292>.
- Walsh K, Haggerty JM, Doane MP, Hansen JJ, Morris MM, Moreira APB, de Oliveira L, Leomil L, Garcia GD, Thompson F, Dinsdale EA. 2017. Auro-biomes are present in the water layer above coral reef benthic macro-organisms. *PeerJ* 5:e3666. <https://doi.org/10.7717/peerj.3666>.
- Spor A, Koren O, Ley R. 2011. Unravelling the effects of the environment and host genotype on the gut microbiome. *Nat Rev Microbiol* 9:279–290. <https://doi.org/10.1038/nrmicro2540>.
- Kueneman JG, Parfrey LW, Woodhams DC, Archer HM, Knight R, McKenzie VJ. 2014. The amphibian skin-associated microbiome across species, space and life history stages. *Mol Ecol* 23:1238–1250. <https://doi.org/10.1111/mec.12510>.
- Adair KL, Douglas AE. 2017. Making a microbiome: the many determinants of host-associated microbial community composition. *Curr Opin Microbiol* 35:23–29. <https://doi.org/10.1016/j.mib.2016.11.002>.
- Apprill A. 2017. Marine animal microbiomes: toward understanding host-microbiome interactions in a changing ocean. *Front Mar Sci* 4:1–9.
- Cinner JE, Huchery C, MacNeil MA, McClanahan TR, Maina J, Maire E, Kittinger JN, Hicks CC, Mora C, Allison EH, D'Agata S, Hoey A, Feary DA, Crowder L, Williams ID, Kulbicki M, Vigliola L, Wantiez L, Edgar G, Stuart-Smith RD, Sandin SA, Green AL, Hardt MJ, Beger M, Friedlander A, Campbell SJ, Holmes KE, Wilson SK, Brokovich E, Brooks AJ, Cruz-Motta JJ, Booth DJ, Chabanet P, Gough C, Tupper M, Ferse SCA, Sumaila UR, Mouillot D. 2016. Bright spots among the world's coral reefs. *Nature* 535:416–419. <https://doi.org/10.1038/nature18607>.
- Hughes TP, Anderson KD, Connolly SR, Heron SF, Kerry JT, Lough JM, Baird AH, Baum JK, Berumen ML, Bridge TC, Claar DC, Eakin CM, Gilmour JP, Graham NAJ, Harrison H, Hobbs J, Hoey AS, Hoogenboom M, Lowe RJ, McCulloch MT, Pandolfi JM, Pratchett M, Schoepf V, Torda G, Wilson SK. 2018. Spatial and temporal patterns of mass bleaching of corals in the Anthropocene. *Science* 359:80–83. <https://doi.org/10.1126/science.aan8048>.
- Dinsdale EA, Rohwer F. 2011. Fish or germs? Microbial dynamics associated with changing trophic structures on coral reefs, p 231–240. *In* Coral reefs: an ecosystem in transition. Springer, New York, NY.
- Kelly LW, Williams GJ, Barott KL, Carlson CA, Dinsdale EA, Edwards RA, Haas AF, Haynes M, Lim YW, McDole T, Nelson CE, Sala E, Sandin SA, Smith JE, Vermeij MJA, Youle M, Rohwer F. 2014. Local genomic adaptation of coral reef-associated microbiomes to gradients of natural variability and anthropogenic stressors. *Proc Natl Acad Sci U S A* 111:10227–10232. <https://doi.org/10.1073/pnas.1403319111>.
- Haas AF, Fairoz MFM, Kelly LW, Nelson CE, Dinsdale EA, Edwards RA, Giles S, Hatay M, Hisakawa N, Knowles B, Lim YW, Maughan H, Pantos O, Roach TNF, Sanchez SE, Silveira CB, Sandin S, Smith JE, Rohwer F. 2016. Global microbialization of coral reefs. *Nat Microbiol* 1:1–7. <https://doi.org/10.1038/nmicrobiol.2016.42>.
- Dinsdale EA, Pantos O, Smriga S, Edwards RA, Angly F, Wegley L, Hatay M, Hall D, Brown E, Haynes M, Knowles B, Lim YW, Maughan H, Pantos O, Roach TNF, Sanchez SE, Silveira CB, Sandin S, Smith JE, Rohwer F. 2008. Microbial ecology of four coral atolls in the Northern Line Islands. *PLoS One* 3:e1584. <https://doi.org/10.1371/journal.pone.0001584>.
- Huggett MJ, Apprill A. 2019. Coral microbiome database: integration of sequences reveals high diversity and relatedness of coral-associated microbes. *Environ Microbiol Rep* 11:372–385. <https://doi.org/10.1111/1758-2229.12686>.
- Rohwer F, Seguritan V, Azam F, Knowlton N. 2002. Diversity and distribution of coral-associated bacteria. *Mar Ecol Prog Ser* 243:1–10. <https://doi.org/10.3354/meps243001>.
- Wegley L, Edwards R, Rodriguez-Brito B, Liu H, Rohwer F. 2007. Metagenomic analysis of the microbial community associated with the

- coral *Porites astreoides*. *Environ Microbiol* 9:2707–2719. <https://doi.org/10.1111/j.1462-2920.2007.01383.x>.
18. Siboni N, Ben-Dov E, Sivan A, Kushmaro A. 2008. Global distribution and diversity of coral-associated Archaea and their possible role in the coral holobiont nitrogen cycle. *Environ Microbiol* 10:2979–2990. <https://doi.org/10.1111/j.1462-2920.2008.01718.x>.
 19. Raina JB, Tapiolas DM, Forêt S, Lutz A, Abrego D, Ceh J, Seneca FO, Clode PL, Bourne DG, Willis BL, Motti CA. 2013. DMSP biosynthesis by an animal and its role in coral thermal stress response. *Nature* 502: 677–680. <https://doi.org/10.1038/nature12677>.
 20. Rädicker N, Pogoreutz C, Voolstra CR, Wiedenmann J, Wild C. 2015. Nitrogen cycling in corals: the key to understanding holobiont functioning? *Trends Microbiol* 23:490–497. <https://doi.org/10.1016/j.tim.2015.03.008>.
 21. Ritchie KB. 2006. Regulation of microbial populations by coral surface mucus and mucus-associated bacteria. *Mar Ecol Prog Ser* 322:1–14. <https://doi.org/10.3354/meps322001>.
 22. Shnit-Orland M, Kushmaro A. 2009. Coral mucus-associated bacteria: a possible first line of defense. *FEMS Microbiol Ecol* 67:371–380. <https://doi.org/10.1111/j.1574-6941.2008.00644.x>.
 23. Peixoto RS, Rosado PM, Leite DC, Rosado AS, Bourne DG. 2017. Beneficial microorganisms for corals (BMC): proposed mechanisms for coral health and resilience. *Front Microbiol* 8:1–16.
 24. Furby KA, Apprill A, Cervino JM, Ossolinski JE, Hughen KA. 2014. Incidence of lesions on Fungiidae corals in the eastern Red Sea is related to water temperature and coastal pollution. *Mar Environ Res* 98:29–38. <https://doi.org/10.1016/j.marenvres.2014.04.002>.
 25. Vega Thurber RL, Burkepile DE, Fuchs C, Shantz AA, McMinds R, Zaneveld JR. 2014. Chronic nutrient enrichment increases prevalence and severity of coral disease and bleaching. *Glob Chang Biol* 20:544–554. <https://doi.org/10.1111/gcb.12450>.
 26. Garren M, Raymundo L, Guest J, Harvell CD, Azam F. 2009. Resilience of coral-associated bacterial communities exposed to fish farm effluent. *PLoS One* 4:e7319. <https://doi.org/10.1371/journal.pone.0007319>.
 27. Thurber RV, Willner-Hall D, Rodriguez-Mueller B, Desnues C, Edwards RA, Angly F, Dinsdale E, Kelly L, Rohwer F. 2009. Metagenomic analysis of stressed coral holobionts. *Environ Microbiol* 11:2148–2163. <https://doi.org/10.1111/j.1462-2920.2009.01935.x>.
 28. Meron D, Atias E, Kruh LI, Elifant H, Minz D, Fine M, Banin E. 2011. The impact of reduced pH on the microbial community of the coral *Acropora eurytoma*. *ISME J* 5:51–60. <https://doi.org/10.1038/ismej.2010.102>.
 29. Zaneveld JR, Burkepile DE, Shantz AA, Pritchard CE, McMinds R, Payet JP, Welsh R, Correa AMS, Lemoine NP, Rosales S, Fuchs C, Maynard JA, Thurber RV. 2016. Overfishing and nutrient pollution interact with temperature to disrupt coral reefs down to microbial scales. *Nat Commun* 7:11833–11812. <https://doi.org/10.1038/ncomms11833>.
 30. Gissi F, Reichelt-Brushett AJ, Chariton AA, Stauber JL, Greenfield P, Humphrey C, Salmon M, Stephenson SA, Cresswell T, Jolley DF. 2019. The effect of dissolved nickel and copper on the adult coral *Acropora muricata* and its microbiome. *Environ Pollut* 250:792–806. <https://doi.org/10.1016/j.envpol.2019.04.030>.
 31. Tracy AM, Koren O, Douglas N, Weil E, Harvell DC. 2015. Persistent shifts in Caribbean coral microbiota are linked to the 2010 warm thermal anomaly. *Environ Microbiol Rep* 7:471–479. <https://doi.org/10.1111/1758-2229.12274>.
 32. Maynard J, van Hooidonk R, Eakin CM, Puotinen M, Garren M, Williams G, Heron SF, Lamb J, Weil E, Willis B, Harvell CD. 2015. Projections of climate conditions that increase coral disease susceptibility and pathogen abundance and virulence. *Nat Clim Chang* 5:688–694. <https://doi.org/10.1038/nclimate2625>.
 33. McDewitt-Irwin JM, Baum JK, Garren M, Vega Thurber RL. 2017. Responses of coral-associated bacterial communities to local and global stressors. *Front Mar Sci* 4:1–16.
 34. Fitt WK, Brown BE, Warner ME, Dunne RP. 2001. Coral bleaching: interpretation of thermal tolerance limits and thermal thresholds in tropical corals. *Coral Reefs* 20:51–65. <https://doi.org/10.1007/s003380100146>.
 35. Lough JM. 2012. Small change, big difference: sea surface temperature distributions for tropical coral reef ecosystems, 1950–2011. *J Geophys Res Ocean* 117:C09018. <https://doi.org/10.1029/2012JC008199>.
 36. Roth MS. 2014. The engine of the reef: photobiology of the coral-algal symbiosis. *Front Microbiol* 5:1–22.
 37. Warner ME, Fitt WK, Schmidt GW. 1996. The effects of elevated temperature on the photosynthetic efficiency of zooxanthellae in hospite from four different species of reef coral: a novel approach. *Plant Cell Environ* 19: 291–299. <https://doi.org/10.1111/j.1365-3040.1996.tb00251.x>.
 38. Harvell D, Jordán-Dahlgren E, Merkel S, Rosenberg E, Raymundo L, Smith G, Weil E, Willis B. 2007. Coral disease, environmental drivers, and the balance between coral and microbial associates. *Oceanography* 20:172–195. <https://doi.org/10.5670/oceanog.2007.91>.
 39. Croquer A, Weil E. 2009. Changes in Caribbean coral disease prevalence after the 2005 bleaching event. *Dis Aquat Organ* 87:33–43. <https://doi.org/10.3354/dao02164>.
 40. Ban SS, Graham NAJ, Connolly SR. 2013. Relationships between temperature, bleaching and white syndrome on the Great Barrier Reef. *Coral Reefs* 32:1–12. <https://doi.org/10.1007/s00338-012-0944-6>.
 41. Willis BL, Page CA, Dinsdale EA. 2004. Coral disease on the great barrier reef, p 69–104. In Rosenberg E, Loya Y (ed), *Coral health and disease*. Springer, Berlin, Germany.
 42. Dinsdale EA. 2002. Abundance of black-band disease on corals from one location on the Great Barrier Reef: a comparison with abundance in the Caribbean region, p 1239–1243. In *Proceedings of the Ninth International Coral Reef Symposium*, Bali, 23–27 October 2000.
 43. Bourne DG, Morrow KM, Webster NS. 2016. Insights into the coral microbiome: underpinning the health and resilience of reef ecosystems. *Annu Rev Microbiol* 70:317–340. <https://doi.org/10.1146/annurev-micro-102215-095440>.
 44. Pollock FJ, McMinds R, Smith S, Bourne DG, Willis BL, Medina M, Thurber RV, Zaneveld JR. 2018. Coral-associated bacteria demonstrate phyllosymbiosis and cophylogeny. *Nat Commun* 9:4921. <https://doi.org/10.1038/s41467-018-07275-x>.
 45. Apprill A, Weber LG, Santoro AE. 2016. Distinguishing between microbial habitats unravels ecological complexity in coral microbiomes. *mSystems* 1:e00143-16. <https://doi.org/10.1128/mSystems.00143-16>.
 46. Sharp KH, Pratte ZA, Kerwin AH, Rotjan RD, Stewart FJ. 2017. Season, but not symbiont state, drives microbiome structure in the temperate coral *Astrangia poculata*. *Microbiome* 5:120. <https://doi.org/10.1186/s40168-017-0329-8>.
 47. Ziegler M, Seneca FO, Yum LK, Palumbi SR, Voolstra CR. 2017. Bacterial community dynamics are linked to patterns of coral heat tolerance. *Nat Commun* 8:14213–14218. <https://doi.org/10.1038/ncomms14213>.
 48. Pantos O, Bongaerts P, Dennis PG, Tyson GW, Hoegh-Guldberg O. 2015. Habitat-specific environmental conditions primarily control the microbiomes of the coral *Seriatopora hystrix*. *ISME J* 9:1916–1927. <https://doi.org/10.1038/ismej.2015.3>.
 49. Krediet CJ, Ritchie KB, Paul VJ, Teplitski M. 2013. Coral-associated micro-organisms and their roles in promoting coral health and thwarting diseases. *Proc Biol Sci* 280:20122328. <https://doi.org/10.1098/rspb.2012.2328>.
 50. Sweet MJ, Bulling MT. 2017. On the importance of the microbiome and pathobiome in coral health and disease. *Front Mar Sci* 4:1–11.
 51. Rypien KL, Ward JR, Azam F. 2010. Antagonistic interactions among coral-associated bacteria. *Environ Microbiol* 12:28–39. <https://doi.org/10.1111/j.1462-2920.2009.02027.x>.
 52. Welsh RM, Rosales SM, Zaneveld JR, Payet JP, McMinds R, Hubbs SL, Thurber R. 2017. Alien versus predator: bacterial challenge alters coral microbiomes unless controlled by *Halobacteriovorax* predators. *PeerJ* 5:e3315. <https://doi.org/10.7717/peerj.3315>.
 53. Lin Q, De Vrieze J, Li J, Li X. 2016. Temperature affects microbial abundance, activity and interactions in anaerobic digestion. *Bioresour Technol* 209:228–236. <https://doi.org/10.1016/j.biortech.2016.02.132>.
 54. Fujimoto M, Lovett B, Angoshtari R, Nirenberg P, Loch TP, Scribner KT, Marsh TL. 2018. Antagonistic interactions and biofilm forming capabilities among bacterial strains isolated from the egg surfaces of lake sturgeon (*Acipenser fulvescens*). *Microb Ecol* 75:22–37. <https://doi.org/10.1007/s00248-017-1013-z>.
 55. Ratkowsky DA, Olley J, McMeekin TA, Ball A. 1982. Relationship between temperature and growth rate of bacterial cultures. *J Bacteriol* 149:1–5. <https://doi.org/10.1128/JB.149.1.1-5.1982>.
 56. Davey KR. 1989. A predictive model for combined temperature and water activity on microbial growth during the growth phase. *J Appl Bacteriol* 67:483–488. <https://doi.org/10.1111/j.1365-2672.1989.tb02519.x>.
 57. Rosso L, Lobry JR, Flandrois J-P. 1993. An unexpected correlation between cardinal temperatures of microbial growth highlighted by a new model. *J Theor Biol* 162:447–463. <https://doi.org/10.1006/jtbi.1993.1099>.
 58. Rosso L, Lobry JR, Bajard S, Flandrois JP. 1995. Convenient model to describe the combined effects of temperature and pH on microbial

- growth. *Appl Environ Microbiol* 61:610–616. <https://doi.org/10.1128/AEM.61.2.610-616.1995>.
59. Vaidya NK, Wahl LM. 2015. Avian influenza dynamics under periodic environmental conditions. *SIAM J Appl Math* 75:443–467. <https://doi.org/10.1137/140966642>.
 60. Marino S, Baxter NT, Huffnagle GB, Petrosino JF, Schloss PD. 2014. Mathematical modeling of primary succession of murine intestinal microbiota. *Proc Natl Acad Sci U S A* 111:439–444. <https://doi.org/10.1073/pnas.1311322111>.
 61. Dam P, Fonseca LL, Konstantinidis KT, Voit EO. 2016. Dynamic models of the complex microbial metapopulation of Lake Mendota. *NPJ Syst Biol Appl* 2:16007. <https://doi.org/10.1038/npsba.2016.7>.
 62. Dinsdale EA, Edwards RA, Hall D, Angly F, Breitbart M, Brulc JM, Furlan M, Desnues C, Haynes M, Li L, McDaniel L, Moran MA, Nelson KE, Nilsson C, Olson R, Paul J, Brito BR, Ruan Y, Swan BK, Stevens R, Valentine DL, Thurber RV, Wegley L, White BA, Rohwer F. 2008. Functional metagenomic profiling of nine biomes. *Nature* 452:629–632. <https://doi.org/10.1038/nature06810>.
 63. Dinsdale EA, Edwards RA, Bailey BA, Tuba I, Akhter S, McNair K, Schmieder R, Apkarian N, Creek M, Guan E, Hernandez M, Isaacs K, Peterson C, Regh T, Ponomarenko V. 2013. Multivariate analysis of functional metagenomes. *Front Genet* 4:41. <https://doi.org/10.3389/fgene.2013.00041>.
 64. Haggerty JM, Dinsdale EA. 2017. Distinct biogeographical patterns of marine bacterial taxonomy and functional genes. *Global Ecol Biogeogr* 26:177–190. <https://doi.org/10.1111/geb.12528>.
 65. Fath BD, Scharler UM, Ulanowicz RE, Hannon B. 2007. Ecological network analysis: network construction. *Ecol Modell* 208:49–55. <https://doi.org/10.1016/j.ecolmodel.2007.04.029>.
 66. Steele JA, Countway PD, Xia L, Vigil PD, Beman JM, Kim DY, Chow C-ET, Sachdeva R, Jones AC, Schwalbach MS, Rose JM, Hewson I, Patel A, Sun F, Caron DA, Fuhrman JA. 2011. Marine bacterial, archaeal, and protistan association networks reveal ecological linkages. *ISME J* 5:1414–1425. <https://doi.org/10.1038/ismej.2011.24>.
 67. Deng Y, Jiang Y-H, Yang Y, He Z, Luo F, Zhou J. 2012. Molecular ecological network analyses. *BMC Bioinformatics* 13:113. <https://doi.org/10.1186/1471-2105-13-113>.
 68. Chow C-E, Kim DY, Sachdeva R, Caron DA, Fuhrman JA. 2014. Top-down controls on bacterial community structure: microbial network analysis of bacteria, T4-like viruses, and protists. *ISME J* 8:816–829. <https://doi.org/10.1038/ismej.2013.199>.
 69. Wang Y, Zhang R, Zheng Q, Deng Y, Van Nostrand JD, Zhou J, Jiao N. 2016. Bacterioplankton community resilience to ocean acidification: evidence from microbial network analysis. *ICES J Mar Sci* 73:865–875. <https://doi.org/10.1093/icesjms/fsv187>.
 70. Layeghifard M, Hwang DM, Guttman DS. 2017. Disentangling interactions in the microbiome: a network perspective. *Trends Microbiol* 25:217–228. <https://doi.org/10.1016/j.tim.2016.11.008>.
 71. Röttgers L, Faust K. 2018. From hairballs to hypotheses: biological insights from microbial networks. *FEMS Microbiol Rev* 42:761–780. <https://doi.org/10.1093/femsre/fuy030>.
 72. Smith SR, De Putron S, Murdoch TJJ, Pitt JM, Nagelkerken I. 2013. Biology and ecology of corals on the Bermuda platform, p 135–151. *In* Sheppard CRC (ed), *Coral reefs of the United Kingdom overseas territories*. Springer, New York, NY.
 73. Borgatti SP. 2005. Centrality and network flow. *Soc Networks* 27:55–71. <https://doi.org/10.1016/j.socnet.2004.11.008>.
 74. Freeman LC. 1977. A set of measures of centrality based on betweenness. *Sociometry* 40:35–41. <https://doi.org/10.2307/3033543>.
 75. De Putron SJ, Smith SR. 2011. Planula release and reproductive seasonality of the scleractinian coral *Porites astreoides* in Bermuda, a high-latitude reef. *BMS* 87:75–90. <https://doi.org/10.5343/bms.2009.1027>.
 76. Courtney TA, Lebrato M, Bates NR, Collins A, De Putron SJ, Garley R, Johnson R, Molinero JC, Noyes TJ, Sabine CL, Andersson AJ. 2017. Environmental controls on modern scleractinian coral and reef-scale calcification. *Sci Adv* 3:e1701356. <https://doi.org/10.1126/sciadv.1701356>.
 77. Zaneveld JR, McMinds R, Thurber RV. 2017. Stress and stability: applying the Anna Karenina principle to animal microbiomes. *Nat Microbiol* 2. <https://doi.org/10.1038/nmicrobiol.2017.121>.
 78. Pratte ZA, Richardson LL. 2018. Microbiome dynamics of two differentially resilient corals. *Dis Aquat Organ* 131:213–226. <https://doi.org/10.3354/dao03289>.
 79. Chu ND, Vollmer SV. 2016. Caribbean corals house shared and host-specific microbial symbionts over time and space. *Environ Microbiol Rep* 8:493–500. <https://doi.org/10.1111/1758-2229.12412>.
 80. Webster NS, Soo R, Cobb R, Negri AP. 2011. Elevated seawater temperature causes a microbial shift on crustose coralline algae with implications for the recruitment of coral larvae. *ISME J* 5:759–770. <https://doi.org/10.1038/ismej.2010.152>.
 81. Lee STM, Davy SK, Tang S-L, Fan T-Y, Kench PS. 2015. Successive shifts in the microbial community of the surface mucus layer and tissues of the coral *Acropora muricata* under thermal stress. *FEMS Microbiol Ecol* 91:fiv142. <https://doi.org/10.1093/femsec/fiv142>.
 82. Glasl B, Bourne DG, Frade PR, Thomas T, Schaffelke B, Webster NS. 2019. Microbial indicators of environmental perturbations in coral reef ecosystems. *Microbiome* 7:94. <https://doi.org/10.1186/s40168-019-0705-7>.
 83. Smith SR, Sarkis S, Murdoch TJJ, Croquer A, Bates NR, Johnson RJ, De Putron S, Andersson AJ. 2013. Threats to coral reefs of Bermuda, p 173–188. *In* Sheppard CRC (ed), *Coral reefs of the United Kingdom overseas territories*. Springer, New York, NY.
 84. Pizzetti I, Schulz F, Tynl T, Fuchs BM, Amann R, Horn M, Fazi S. 2016. Chlamydial seasonal dynamics and isolation of “*Candidatus Neptunochlamydia vexilliferae*” from a Tyrrhenian coastal lake. *Environ Microbiol* 18:2405–2417. <https://doi.org/10.1111/1462-2920.13111>.
 85. Silveira CB, Cavalcanti GS, Walter JM, Silva-Lima AW, Dinsdale EA, Bourne DG, Thompson CC, Thompson FL. 2017. Microbial processes driving coral reef organic carbon flow. *FEMS Microbiol Rev* 41:575–595. <https://doi.org/10.1093/femsre/fux018>.
 86. Berry D, Widder S. 2014. Deciphering microbial interactions and detecting keystone species with co-occurrence networks. *Front Microbiol* 5:219. <https://doi.org/10.3389/fmicb.2014.00219>.
 87. Baldassano SN, Bassett DS. 2016. Topological distortion and reorganized modular structure of gut microbial co-occurrence networks in inflammatory bowel disease. *Sci Rep* 6:26087. <https://doi.org/10.1038/srep26087>.
 88. Estrada-Peña A, Cabezas-Cruz A, Pollet T, Vayssier-Taussat M, Cosson J-F. 2018. High throughput sequencing and network analysis disentangle the microbial communities of ticks and hosts within and between ecosystems. *Front Cell Infect Microbiol* 8:236. <https://doi.org/10.3389/fcimb.2018.00236>.
 89. Haas AF, Nelson CE, Rohwer F, Wegley-Kelly L, Quistad SD, Carlson CA, Leichter JJ, Hatay M, Smith JE. 2013. Influence of coral and algal exudates on microbially mediated reef metabolism. *PeerJ* 1:e108. <https://doi.org/10.7717/peerj.108>.
 90. Tout J, Jeffries TC, Webster NS, Stocker R, Ralph PJ, Seymour JR. 2014. Variability in microbial community composition and function between different niches within a coral reef. *Microb Ecol* 67:540–552. <https://doi.org/10.1007/s00248-013-0362-5>.
 91. Goodbody-Gringley G, Wong KH, Becker DM, Glennon K, de Putron SJ. 2018. Reproductive ecology and early life history traits of the brooding coral, *Porites astreoides*, from shallow to mesophotic zones. *Coral Reefs* 37:483–494. <https://doi.org/10.1007/s00338-018-1673-2>.
 92. de Putron SJ, Lawson JM, White KQL, Costa MT, Geronimus MVB, McCarthy A. 2017. Variation in larval properties of the Atlantic brooding coral *Porites astreoides* between different reef sites in Bermuda. *Coral Reefs* 36:383–393. <https://doi.org/10.1007/s00338-016-1527-8>.
 93. Glasl B, Webster NS, Bourne DG. 2017. Microbial indicators as a diagnostic tool for assessing water quality and climate stress in coral reef ecosystems. *Mar Biol* 164:1–18. <https://doi.org/10.1007/s00227-017-3097-x>.
 94. Mera H, Bourne DG. 2018. Disentangling causation: complex roles of coral-associated microorganisms in disease. *Environ Microbiol* 20: 431–449. <https://doi.org/10.1111/1462-2920.13958>.
 95. Warner ME, Fitt WK, Schmidt GW. 1999. Damage to photosystem II in symbiotic dinoflagellates: a determinant of coral bleaching. *Proc Natl Acad Sci U S A* 96:8007–8012. <https://doi.org/10.1073/pnas.96.14.8007>.
 96. Kemp DW, Oakley CA, Thornhill DJ, Newcomb LA, Schmidt GW, Fitt WK. 2011. Catastrophic mortality on inshore coral reefs of the Florida Keys due to severe low-temperature stress. *Glob Change Biol* 17:3468–3477. <https://doi.org/10.1111/j.1365-2486.2011.02487.x>.
 97. Roth MS, Goerick R, Deheyn DD. 2012. Cold induces acute stress but heat is ultimately more deleterious for the reef-building coral *Acropora yongei*. *Sci Rep* 2:240. <https://doi.org/10.1038/srep00240>.
 98. Brown BE, Bythell JC. 2005. Perspectives on mucus secretion in reef corals. *Mar Ecol Prog Ser* 296:291–309. <https://doi.org/10.3354/meps296291>.
 99. Glasl B, Herndl GJ, Frade PR. 2016. The microbiome of coral surface mucus has a key role in mediating holobiont health and survival upon disturbance. *ISME J* 10:2280–2292. <https://doi.org/10.1038/ismej.2016.9>.
 100. Doane MP, Haggerty JM, Kacev D, Papudeshi B, Dinsdale EA. 2017. The

- skin microbiome of the common thresher shark (*Alopias vulpinus*) has low taxonomic and gene function β -diversity. *Environ Microbiol Rep* 9:357–373. <https://doi.org/10.1111/1758-2229.12537>.
101. Cavalcanti GS, Shukla P, Morris M, Ribeiro B, Foley M, Doane MP, Thompson CC, Edwards MS, Dinsdale EA, Thompson FL. 2018. Rhodoliths holobionts in a changing ocean: host-microbe interactions mediate coralline algae resilience under ocean acidification. *BMC Genomics* 19:–13. <https://doi.org/10.1186/s12864-018-5064-4>.
 102. Minich JJ, Morris MM, Brown M, Doane M, Edwards MS, Michael TP, Dinsdale EA. 2018. Elevated temperature drives kelp microbiome dysbiosis, while elevated carbon dioxide induces water microbiome disruption. *PLoS One* 13:e0192772–23. <https://doi.org/10.1371/journal.pone.0192772>.
 103. Edwards RA, Haggerty JM, Cassman N, Busch JC, Aguinaldo K, Chinta S, Vaughn MH, Morey R, Harkins TT, Teiling C, Fredrikson K, Dinsdale EA. 2013. Microbes, metagenomes, and marine mammals: enabling the next generation of scientist to enter the genomic era. *BMC Genomics* 14:600. <https://doi.org/10.1186/1471-2164-14-600>.
 104. Hernandez D, François P, Farinelli L, Østerås M, Schrenzel J. 2008. De novo bacterial genome sequencing: millions of very short reads assembled on a desktop computer. *Genome Res* 18:802–809. <https://doi.org/10.1101/gr.072033.107>.
 105. Kozarewa I, Ning Z, Quail MA, Sanders MJ, Berriman M, Turner DJ. 2009. Amplification-free Illumina sequencing-library preparation facilitates improved mapping and assembly of (G+C)-biased genomes. *Nat Methods* 6:291–295. <https://doi.org/10.1038/nmeth.1311>.
 106. Schmieder R, Edwards R. 2011. Quality control and preprocessing of metagenomic datasets. *Bioinformatics* 27:863–864. <https://doi.org/10.1093/bioinformatics/btr026>.
 107. Zhang J, Kobert K, Flouri T, Stamatakis A. 2014. PEAR: a fast and accurate Illumina Paired-End reAd mergeR. *Bioinformatics* 30:614–620. <https://doi.org/10.1093/bioinformatics/btt593>.
 108. Silva GGZ, Cuevas DA, Dutilh BE, Edwards RA. 2014. FOCUS: an alignment-free model to identify organisms in metagenomes using non-negative least squares. *PeerJ* 2:e425. <https://doi.org/10.7717/peerj.425>.
 109. Sczyrba A, Hofmann P, Belmann P, Koslicki D, Janssen S, Dröge J, Gregor I, Majda S, Fiedler J, Dahms E, Bremges A, Fritz A, Garrido-Oter R, Jørgensen TS, Shapiro N, Blood PD, Gurevich A, Bai Y, Turaev D, DeMaere MZ, Chikhi R, Nagarajan N, Quince C, Meyer F, Balvočiūtė M, Hansen LH, et al. 2017. Critical assessment of metagenome interpretation: a benchmark of metagenomics software. *Nat Methods* 14:1063–1071. <https://doi.org/10.1038/nmeth.4458>.
 110. McKinney W. 2011. pandas: a foundational Python library for data analysis and statistics. *Python High Perform Sci Comput* 14:9.
 111. Hagberg A, Swart P, Chult DS. 2008. Exploring network structure, dynamics, and function using NetworkX. Los Alamos National Laboratory, Los Alamos, NM.
 112. Csardi G, Nepusz T. 2006. The igraph software package for complex network research. *InterJournal, Complex Syst* 1695:1–9.
 113. Revelle W. 2011. An overview of the psych package. *Dep Psychol Northwest Univ* 3:1–25.
 114. Bonacich P. 1972. Factoring and weighting approaches to status scores and clique identification. *J Math Sociol* 2:113–120. <https://doi.org/10.1080/0022250X.1972.9989806>.
 115. Bonacich P. 2007. Some unique properties of eigenvector centrality. *Soc Networks* 29:555–564. <https://doi.org/10.1016/j.socnet.2007.04.002>.